Simulation and Experimental Evaluation of a Resonant Magnetic Wireless Power Transfer System for Seawater Operation

M. R. Pereira
INESC TEC
mario.r.pereira@inesctec.pt

H. M. Santos
INESC TEC / FEUP
hugo.m.santos@inesctec.pt

L. M. Pessoa
INESC TEC
luis.m.pessoa@inesctec.pt

H. M. Salgado
INESC TEC / FEUP
hsalgado@inesctec.pt

Abstract—The use of high efficiency resonant coupling wireless power systems for subsea operations is here considered for the charging of autonomous underwater vehicles. In this paper, two architectures based on two different inductors are analysed for their potential as resonant wireless power couplers. Both systems were designed and optimised through electromagnetic 3D simulations, upon which two prototypes were constructed and measured. Efficiencies as high as 75% for distances up to 5 cm were achieved on experimental testing.

I. INTRODUCTION

The employment of fixed and mobile sensors within underwater environments is nowadays a standard practice in several fields of activity, namely, environmental monitoring as well as in the inspection of permanent subsea infrastructures. Sensors deployed on permanent subsea structures or on the seabed generally lack cabled connections, and therefore rely on batteries. Approaching these sensors with Autonomous Underwater Vehicles (AUVs) for replenishing their batteries and recovering measurement data is very appealing. However, presently, the most common solution involves the operation of remotely operated vehicles (ROVs), which is very expensive since a support vessel is required and therefore can only be considered for small-scale operations [1]. On the other hand, mobile underwater vehicles such as ROVs or AUVs may carry sensors for underwater sensing in specific missions. In fact, the employment of AUVs is an emerging practice, potentially suitable for large-scale autonomous operation. ENDURE [2] is a project funded by the EEA Grants financial mechanism, that aims to develop an underwater docking station suitable for recharging the batteries of AUVs in remote oceanic locations, paving the way to enable the permanent operation in deep-sea scenarios. The project targets to achieve a simple docking mechanism, a wireless power transfer system and a wireless broadband communications system. Fig. 1 shows a deep-sea operation scenario, including the MARES AUV, which is a highly flexible small-scale AUV developed at INESC TEC, that can be configured to carry specific prototypes and logging systems for experimental evaluation [3]. However, the use of AUVs is limited by the duration of their energy source charge. Hence, there is the need for an energy solution that can support the operation of a number of AUVs within underwater environments for long periods of time. Currently available AUV
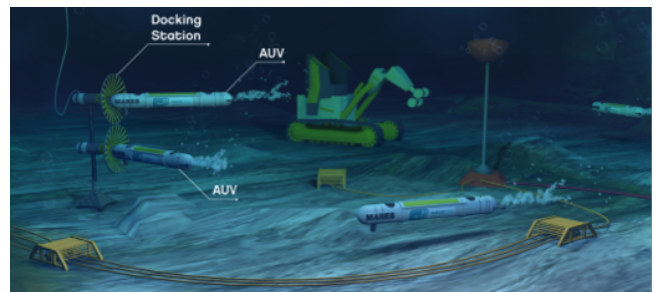

Fig. 1: Docking stations for AUV recharging in a deep-sea operation scenario.

recharging solutions are very complex, typically requiring wet mate connectors [4], which are prone to failure and require frequent maintenance and/or too complex docking mechanisms. As such, these solutions are not appropriate for scaling-up due to the high costs and therefore their usage has been limited. The research on techniques for underwater wireless power transfer has been increasing in the last years, targeting not only the battery charging of AUVs but also wireless powering of underwater sensors. Witricity has released a white paper in 2013 [5] demonstrating the possibility of using resonant magnetic coupling (RMC) through salt water. The authors transferred power across a plastic container filled with water and used a halogen lamp as a load. The authors conclude that a significant power level (up to several kW) may be transferred across a gap of 15 cm with a wireless transfer efficiency in the order of 80%. Inductive coupling is currently the alternative to wet-mate connectors most often seen in the literature. For instance, in [6] the authors describe an underwater wireless power transfer system based on inductive coupling. The efficiency reported is around 90% for a distance of 2 mm. Such small distances however present an operational problem from an AUV manoeuvrability standpoint, as it requires a very precise alignment. In [7], the charging stations are outfitted with alignment cones to overcome this problem. In [8] an underwater WPT system is reported with wireless transfer efficiency of 60% across a gap of 10 cm, using an inductive resonant structure with a size of 25 cm by 25 cm.

This paper is organised as follows. In section II we proceed
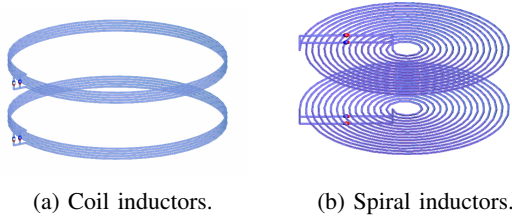
(a) Coil inductors. (b) Spiral inductors.

Fig. 2: Underwater WPT simulation models.

to the analysis and performance comparison of both coil and spiral inductor WPT systems through 3D electromagnetic (EM) simulation. In section III the experimental results are presented and finally in section IV some conclusions are drawn regarding the work presented and some guidelines are proposed for future improvements.

II. SYSTEM DESCRIPTION AND SIMULATION

The heart of any low frequency wireless power system are usually two very large inductors, through which energy is coupled via the magnetic field. In this paper we study two different inductor architectures, namely a coil- and a spiral-based architecture as illustrated in Figure 2. Both inductors have an external diameter of approximately 15 cm and are made out of 1.5 mm thickness magnet copper wire. In both architectures, a parallel tuning capacitor is included to achieve anti-resonance at around 100 KHz, where the system operates optimally using $50\,\Omega$ impedance terminations at both transmitter and load sides. At 100 KHz, the simulated inductance values for the coil and spiral inductors are $8.44\,\mu$H and $16.9\,\mu$H, respectively. The corresponding tuning capacitors are 300 nF for the coils and 150 nF for the spirals. Seawater was considered as the target transfer medium for WPT, nevertheless, simulation and experimental characterisations of both systems for air and fresh water mediums were also conducted.

Figure 3 shows the transmission frequency response for the coil architecture system when the two resonators are placed next to one another. From the plot, we easily see that for distances lower than around 7 cm the $|S_{21}|$ response features two peaks of high value. In this case, the two resonators are said to be over-coupled. For distances above 9 cm, it only shows one peak, and the maximum $|S_{21}|$ value begins to drop with increasing distance. In this case, the resonators are said to be under-coupled. The so-called critical coupling distance is the distance at which the system transitions from over-coupled to under-coupled. At this distance, the $|S_{21}|$ frequency response features only one peak of high $|S_{21}|$, which starts to drop for higher distances (under-coupling). Similar transmission frequency responses can be obtained for the spiral architecture, however, different $|S_{21}|$ peak values and critical coupling distances are obtained.

The two architectures, coil and spiral based inductors, can be compared by means of their efficiency. The power efficiency of the WPT systems can be directly computed from their corresponding transmission frequency response (with $50\,\Omega$
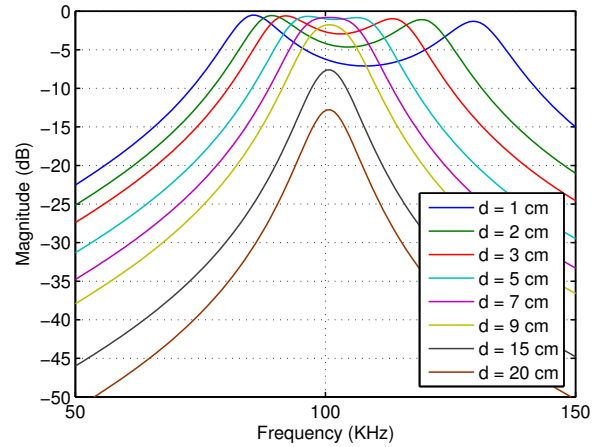

Fig. 3: Simulated transmission frequency response (S_{21}) of the coil architecture, as a function of the distance between inductors.
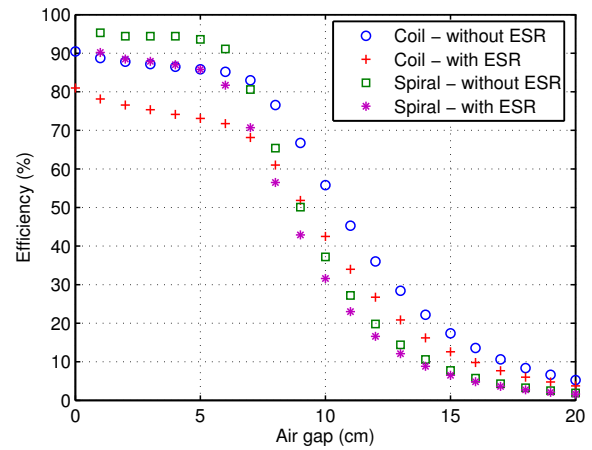

Fig. 4: Auto-tuned efficiency obtained by simulation as a function of distance with and without tuning capacitor losses (ESR$_{\text{coil}}$ = 53 mΩ, ESR$_{\text{spiral}}$ = 106 mΩ).

port impedance for both ports). Hence, the output to input power ratio (power efficiency) at a given frequency is given from the transmission coefficient of the system as the square of the magnitude of the transmission coefficient, i.e., $|S_{21}|^2$.

Figure 4 depicts the efficiency results of simulation the for both the coil and spiral architectures in air by plotting the auto-tuned efficiency as a function of distance. The auto-tuned efficiency is obtained by operating the system at a frequency where the efficiency is maximum. As shown in Figure 3, this corresponds to choosing the frequency where $|S_{21}|$ is maximum for each distance (gap) between the inductors.

The simulation data presented in Figure 4 comprises two pair of results for the efficiency versus air gap of each architecture, one considering an ideal tuning capacitor, i.e., a capacitor without losses, and the other one where the capacitor substrate losses are modelled as an equivalent series
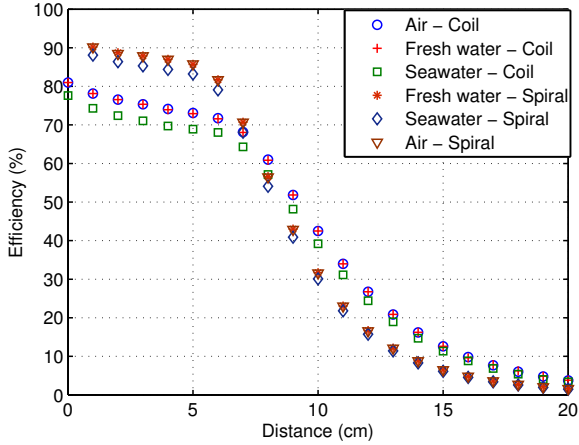
Fig. 5: Simulated auto-tuned efficiency as a function of distance between inductors for air, fresh and seawater mediums
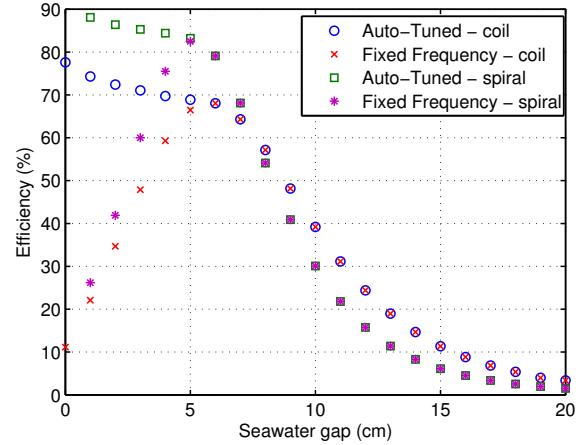.

Fig. 6: Simulated efficiency as a function of the seawater gap for both coil and spiral configurations.

resistance (ESR). Since the ESR lowers the quality factor of the resonators, which is equivalent to an increase energy dissipation with increasing ESR, the results given in Figure 4, show a significant reduction of the efficiency when including the losses of the substrate of the capacitor.

The ESR value for capacitors is given by

$$ESR = \frac{tg\,\delta}{\omega C}, \tag{1}$$

where ω is the angular frequency, C is the capacitance value and $tg\,\delta$ is the dielectric loss tangent of the capacitor.

According to (1), the ESR for the spirals tuning capacitor will be twice that of the coils architecture since it has half the capacitance. Then, on the over-coupled region, we would expect that the efficiency degradation of the spiral system to be higher than that of the coil system. However, from Figure 4 we can actually observe the opposite behaviour. In fact, we see that, when taking into account the capacitor losses in the simulation, the efficiency degradation for the coils is more than twice that of the spirals. The explanation for this has to do with the fact that the coils inductance is significantly lower than that of the spirals. This means that, at the peaks of $|S_{21}|$ the current flowing through the capacitors and consequently through their respective ESRs, is higher for the coils than for the spirals architecture. If the current difference is high enough and because $P = ESR \cdot I^2$, the power dissipated in the coils ESR can in fact be higher than that of the spiral case, even if the ESR is lower. This was in fact verified through simulation, hence the higher efficiency loss for the coil architecture.

In summary, the results in Figure 4 essentially show that in the air environment, the spiral architecture is more efficient than the coil architecture and that the efficiency is highly affected by the ESR of the capacitors. Furthermore, it can be seen that the efficiency remains approximately steady in the over-coupled region, up to 8 cm and 6 cm, for the coil and

(a) Coil inductor.

(b) Spiral inductor.

Fig. 7: Coil an spiral prototypes.

spiral based inductors, respectively. Efficiency falls rapidly for higher gaps, corresponding to the under-coupled region.

The ESR values used on the EM simulation are $53\,\text{m}\Omega$ and $106\,\text{m}\Omega$ for the coil and spiral architectures respectively. These values were calculated through (1) using the loss tangent ($tg\,\delta = 0.01$) provided by the data-sheet of the actual capacitors used on the prototypes. All the simulation results shown from now on shall use these ESR values.

Figure 5 compares the efficiency results of simulation for both coil and spiral architectures considering air, fresh water and seawater as the transfer mediums. Clearly we see that the spiral architecture is the more efficient for all the mediums considered. Furthermore, it becomes clear from the plot that, the efficiency of both architectures is practically unaffected by the different mediums. In fact, the air and fresh water performances are exactly the same. For seawater some efficiency loss is observed for both architectures due to the considerably higher conductivity.

As the main goal for the work presented in this paper is the study of WPT in seawater, Figure 6 depicts the energy transfer efficiency results of simulation for both architectures in seawater. Here we introduce the fixed-frequency efficiency results. Unlike auto-tuned efficiency, fixed-frequency results are obtained by measuring the efficiency at a fixed frequency, usually the resonant frequency so that the peak (maximum)
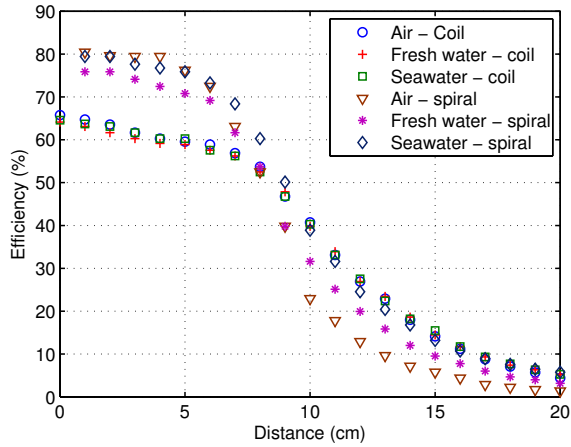
Fig. 8: Auto-tuned measured efficiency as a function of distance between inductors for air, fresh and seawater .

Fig. 9: Efficiency comparison between simulation and experimental results for the coil configuration in seawater.

efficiency always occurs at the critical coupling distance.

From the Figure 6 we conclude that for seawater operation the spiral architecture is about 12% more efficient than the coil architecture.

III. EXPERIMENTAL RESULTS

In order to verify the simulation results, two different prototypes have been constructed and experimentally evaluated in air, fresh water as well as seawater. Figure 7 depicts both prototypes, which were constructed accordingly to the EM simulation models. The coils were constructed by tightly wounding 5 turns of magnet wire around a 15 cm diameter rod. The woundings were fixed in place using hot glue, after which the coils were removed from the rod. In order to assemble the spiral inductor, two white plastic supports with grooves were 3D printed. The spiral was constructed by manually wounding the magnet wire through the grooves of the plastic supports. The magnet wire was then fixed to the plastic supports using hot glue. The tuning capacitors were directly soldered to the terminals of both the coils and the spirals. For the spiral architecture, a single 150 nF capacitor was used, whereas, for the coil architecture two 150 nF capacitors were soldered in parallel in order to obtain the required 300 nF capacitance value. Both the capacitors and the soldered connections were waterproofed with hot glue. In order to perform the spiral architecture measurements, a wooden structure was constructed so that the distance between spirals could be adjusted while keeping both spirals always parallel to each other. The coil architecture measurements where performed by sliding both coils through a 15 cm diameter piece of acrylic, thus ensuring the alignment between coils while adjusting the distance between them.

Figure 8 shows the measured efficiencies as a function of distance between resonators for air, fresh water and seawater mediums. Clearly, we see that the efficiencies for both architectures are barely unaffected by the different mediums as it was previously verified through EM simulation. Additionally,
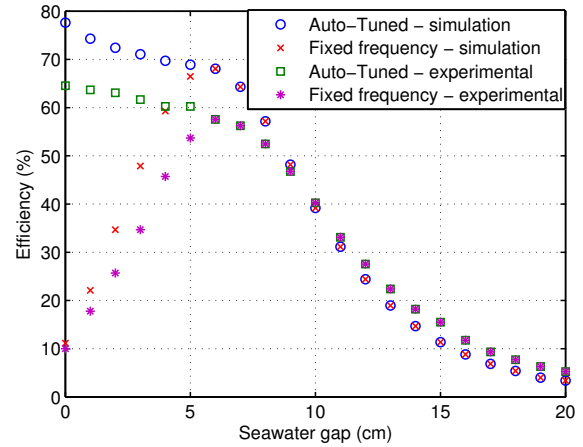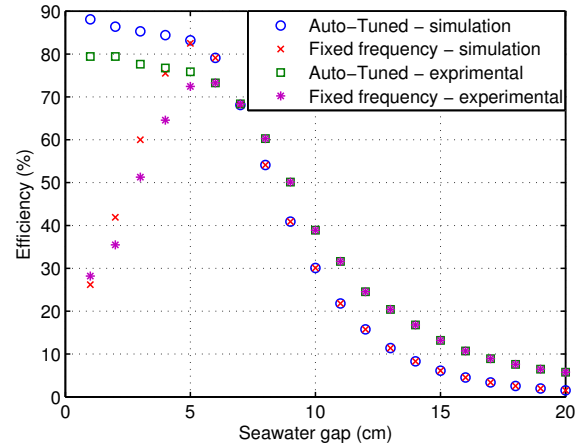

Fig. 10: Efficiency comparison between simulation and experimental results for the spiral configuration in seawater.

it is confirmed that the spiral architecture is the most efficient architecture for all the different mediums.

Comparing Figure 8 with Figure 5 we clearly see an excellent agreement between simulation and experimental results. Both simulation and experimental results for the efficiency show practically the same variation with increasing distance between resonators. There is however, an appreciable difference in the efficiency values within the over-coupled region. The same conclusions can be drawn form Figure 9 and Figure 10, where a direct comparison between the EM simulation and experimental results for the coil and spiral architectures in seawater is presented. An efficiency reduction of 11% and 9% from the simulation to the experimental results is seen for the coil and spiral architectures, respectively. It is our understanding that, this difference between simulation and measurement efficiencies may be explained by poor soldered connections (contact resistance) on the capacitors. Furthermore, the actual ESR values may be higher than those

considered in the simulation. In fact, the accuracy of the loss tangent of the capacitors is not known. Also the conductivity for the magnet wire used to construct both the coils and the spirals is not precisely known, whereas in the simulations, a standard conductivity value for cooper was used. All these factors may explain the discrepancies observed.

Nevertheless, the implemented prototypes still exhibit reasonable high efficiencies, higher than 75% and 60% for the spiral and coil based architectures, respectively, up to a distance of 5 cm.

IV. CONCLUSION

In this paper two different architectures have been evaluated both though simulation and experimentally for three different mediums,i.e., air, fresh water and seawater. In both architectures, high efficient WPT has been successfully achieved.

The experimental results are in good agreement with the simulations results, however a difference of 11% and 9% is verified between the simulation and measurement results for the coil and spiral architectures respectively. Furthermore, it was verified that the spiral architecture is the most efficient architecture for all the different mediums.

Future work will address the improvement of the efficiency of both architectures through additional optimisations, including using higher quality capacitors, i.e., lower ESR. The efficiency degradation resulting from non-aligned resonators will also be addressed.

In conclusion and given both the simulation and experimental results presented in this paper, underwater WPT using magnetic resonance appears to be a promising solution for power transfer in underwater.

REFERENCES

[1] R. B. Wynn, V. A. Huvenne, T. P. Le Bas, B. J. Murton, D. P. Connelly, B. J. Bett, H. A. Ruhl, K. J. Morris, J. Peakall, D. R. Parsons *et al.*, "Autonomous underwater vehicles (auvs): Their past, present and future contributions to the advancement of marine geoscience," *Marine Geology*, vol. 352, pp. 451–468, 2014.

[2] http://endure.inesctec.pt.

[3] N. A. Cruz and A. C. Matos, "The mares auv, a modular autonomous robot for environment sampling," in *OCEANS 2008*. IEEE, 2008, pp. 1–6.

[4] T. Kojiya, F. Sato, H. Matsuki, and T. Sato, "Automatic power supply system to underwater vehicles utilizing non-contacting technology," in *OCEANS'04. MTTS/IEEE TECHNO-OCEAN'04*, vol. 4. IEEE, 2004, pp. 2341–2345.

[5] M. Kesler, "Highly resonant wireless power transferin subsea applications," *WiTricity Corporation*, 2013.

[6] Z.-s. Li, D.-j. Li, L. Lin, and Y. Chen, "Design considerations for electromagnetic couplers in contactless power transmission systems for deep-sea applications," *Journal of Zhejiang University SCIENCE C*, vol. 11, no. 10, pp. 824–834, 2010.

[7] J.-g. Shi, D.-j. Li, and C.-j. Yang, "Design and analysis of an underwater inductive coupling power transfer system for autonomous underwater vehicle docking applications," *Journal of Zhejiang University SCIENCE C*, vol. 15, no. 1, pp. 51–62, 2014.

[8] K. Shizuno, S. Yoshida, M. Tanomura, and Y. Hama, "Long distance high efficient underwater wireless charging system using dielectric-assist antenna," in *Oceans-St. John's, 2014*. IEEE, 2014, pp. 1–3.